Carbonation Conversion of Aqueous Sodium Sulfide to Hydrogen Sulfide

Steven H. Ng,[†] Charles Q. Jia, and W-K. Lu*

Department of Materials Science and Engineering, McMaster University, Hamilton, Ontario, Canada L8S 4L7

In order to control SO_2 emissions, one option is to win metal from sulfide ores under reducing conditions. In this direct reduction process with soda ash as the flux, one of the key steps is the recovery of sulfur from Na_2S. The objective of the present study is to investigate the kinetics of the carbonation conversion of aqueous Na_2S to gaseous H_2S for the purpose of elemental sulfur production. In a reactor which is characterized by continuous operation with respect to gas flow, but batchwise for the liquid phase, three distinct reaction periods were observed. In the second period which is of practical importance, the reaction is first order with respect to bisulfide concentration in solution and first order with respect to CO_2 partial pressure. In this well-mixed system, chemical reactions in solution are extremely fast. The H_2S content in the outgoing gas is high enough for a Claus plant to produce elemental sulfur. Considering the observed negative effect of temperature on the overall reaction, it is likely that the absorption of CO_2 would be one of the rate-limiting step(s).

Figure 1. Experimental setup: A, CO_2 cylinder; B, N_2 cylinder; C, needle valves; D, mass flow controller; E, reactor (33-mm diameter) with a fritted cylinder (12-mm diameter, 20-mm long); F, water path; G, circulator; H, hydrogen sulfide absorbers.

I. Introduction

Of the several air pollutants that contribute to acid rain, sulfur oxides (mainly sulfur dioxide) have received special attention due to their large and increasing quantity on a global basis. Conventional processes for the winning of metals from sulfide concentrates generally involve roasting and converting (*1, 2*), i.e., the oxidation of metal sulfide by air or oxygen. As an alternative approach to win metal from its sulfide ore, carbothermic reduction in the presence of soda ash rather than oxidation has been considered (*3*). Hydrogen sulfide may be generated and converted to elemental sulfur for storage or shipping to far away markets. The main potential advantage of this new reduction process of sulfide concentrates is the prevention of sulfur dioxide formation, hence emission to the atmosphere (*4*).

Carbonation conversion of aqueous sodium sulfide, i.e., with CO_2 gas, is particularly favorable since CO_2 is readily available in the flue gas of carbothermic reduction furnaces. This process has been of considerable interest in the past and has been described in the patent literature (*5*). However, relevant data concerning this system are very limited (*6, 7*), particularly in regard to reaction kinetics, which is crucial for industrial reactor design. The major objective of this research, therefore, is to study the reaction kinetics and mechanisms.

II. Experimental Considerations

As shown in Figure 1, the desorption of H_2S from aqueous Na_2S solution enhanced by CO_2 bubbling was studied with the use of a bubble column equipped with a fine porosity (40–60 μm) dispersion cylinder as the reactor. The solution depth was 165 mm without gas bubbling.

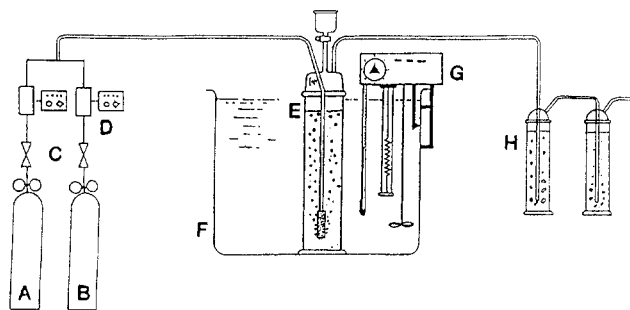† Present address: RACAL Filter Technology Ltd., Brockvill, Ontario, Canada K6V 5V8.

The reactor was submerged in a water bath whose temperature was controlled within 0.5 °C by a Brinkmann circulator (Model IC-2). Coleman instrumental-grade CO_2 gas, mass flow rate accurately controlled by a Mathesson mass flowmeter (Model 8259,SP-1734), was delivered to the aqueous solution in the reactor. After passing through the solution in the gas washing bottles containing alkaline sodium nitroprusside, the reacted gas finally exited to the fume hood exhaust. The pH value of the solution was measured by a Fisher Accumet pH meter (Model 140).

The BDH reagent-grade $Na_2S \cdot 9H_2O$ crystals were used to prepare the stock solution. Its concentration was then determined by iodometric titration with excess potassium iodate and back-titration with sodium thiosulfate. Reagent-grade $NaHCO_3$ crystals, potassium iodate, and $Na_2S_2O_3$ were also used.

All experiments were isothermal and started off with approximately the same Na_2S concentration but were terminated after different reaction times. The amount of residual sulfide in solution ($S^{2-}_{(aq)}$, $HS^-_{(aq)}$, and $H_2S_{(aq)}$) could, therefore, be directly measured (*8*). This gave the concentration of sulfide in solution as a function of time and, hence, enabled the determination of the dependence of the H_2S desorption rate on sulfide concentration.

The extent of the gaseous H_2S generation reaction was determined by measuring the difference of sulfide content of the solution before and after reaction. Accordingly, at the termination of the reaction, the solution was diluted to minimize further reaction (*9*).

III. Experimental Results

The dependence of Na_2S conversion rate on the reaction temperature, the CO_2 flow rate, and the partial pressure of CO_2 are shown in Figures 2–4, respectively. For the pressurized systems, the H_2S absorbers were replaced by a pressure gauge and a gas regulator (Mathson Model 3332). Due to equipment constraint, reactions at two higher pressures of 129 kPa (4 psig) and 163 kPa (9 psig) were studied. It was noticed that it took the reaction system about 2 min to reach 129 kPa and 4 min to 163 kPa.

At first glance Figure 5 might suggest that pressurization has little effect on the overall conversion rate of Na_2S as compared to that of the atmospheric system. However,
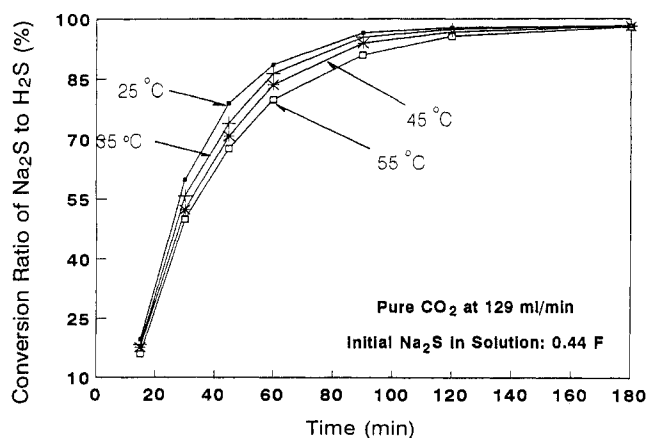
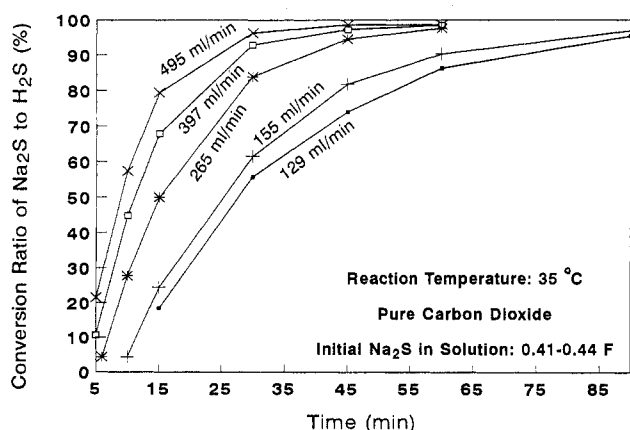**Figure 2.** Percent conversion of Na_2S to H_2S vs reaction time at different temperatures.

Figure 3. Percent conversion of Na_2S to H_2S vs reaction time at different CO_2 flow rates.
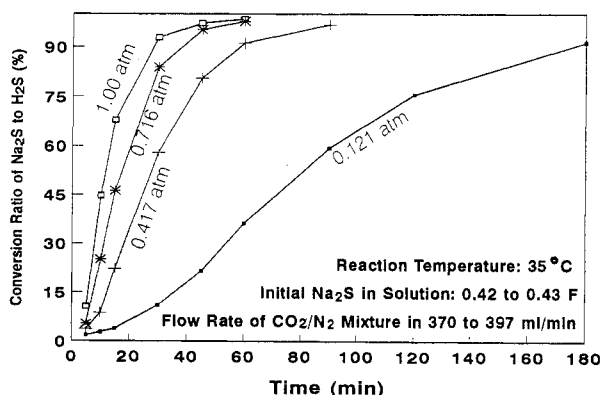

Figure 4. Percent conversion of Na_2S to H_2S vs reaction time with different CO_2 partial pressures.

the gas–liquid interfacial area decreases according to the ideal gas law while the mass flow rate of gas and volume of solution in the reactor are kept constant. Hence, Figure 5 implies that the reaction rate, in terms of the amount of sodium sulfide reacted per unit area of gas–liquid interface and per unit time, increased in a pressurized reactor.

A high-speed motion picture camera was used to photograph the reaction vessel in an attempt to estimate bubble size distribution (4). It has been found that the size of bubbles tended to increase with the increase of volumetric flow rate of gas. The size of bubbles was from 0.3 to 1.6 mm in diameter, mainly from 0.5 to 1.0 mm. Based on the estimated bubble size distribution and
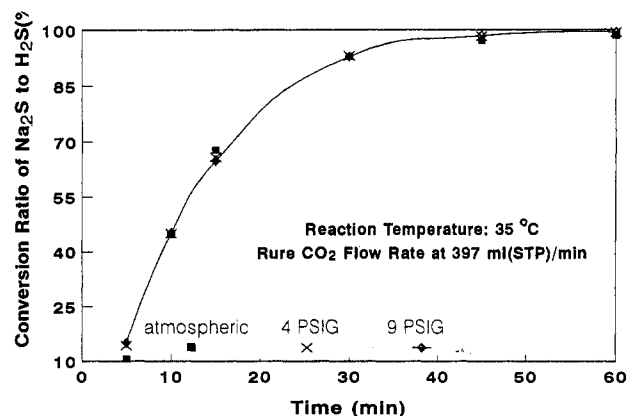

Figure 5. Percent conversion of Na_2S to H_2S vs reaction time in pressurized system.

number density, the interfacial area per unit volume of solution may be determined by

$$A_{g/l} = \left(\frac{\text{total surface area of bubbles}}{\text{total vol of bubbles}}\right)\left(\frac{\text{gas holdup vol}}{\text{vol of solution}}\right) \quad (1)$$
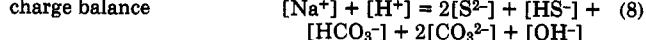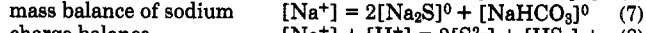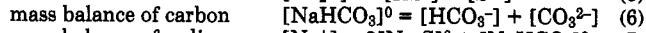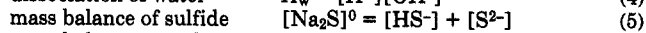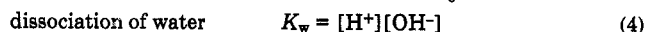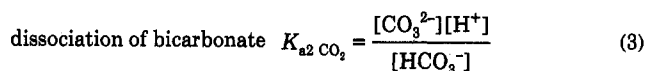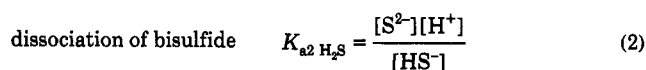
This quantity will be used in the kinetic expression to be shown later.

IV. Discussion

Ionic Composition of Solution. It is anticipated that heterogeneous reactions in this system are more likely to be rate-limiting in view of the fact that reactions in the liquid phase are extremely fast. An attempt was made to compute the concentration of ions based on the thermodynamic data (10–12). There are seven unknowns, [HS⁻], [S²⁻], [HCO₃⁻], [CO₃²⁻], [H⁺], [OH⁻], and [Na⁺]; therefore, seven constraints were required. The dissociation reactions of dissolved H_2S, CO_2, and H_2O, which may be assumed to be in equilibrium because they involve only the transfer of a proton, provide three equations. The mass balance of sulfur, carbon, and sodium in solution and the charge balance among ions are these additional equations used in the computation (4). Details are summarized in Table I.

The results of computation for the initial state, i.e., before the bubbling of CO_2, which may be compared with available data such as pH value are very successful. For a solution of 0.418 F Na_2S and 0.600 F $NaHCO_3$ at 25 °C, the calculated concentration of H⁺ ions is 2.055×10^{-11} M,

Table I. Equations Used in Computation of Concentration of Ions[a]

dissociation of bisulfide	$K_{a2\,H_2S} = \dfrac{[S^{2-}][H^+]}{[HS^-]}$	(2)
dissociation of bicarbonate	$K_{a2\,CO_2} = \dfrac{[CO_3^{2-}][H^+]}{[HCO_3^-]}$	(3)
dissociation of water	$K_w = [H^+][OH^-]$	(4)
mass balance of sulfide	$[Na_2S]^0 = [HS^-] + [S^{2-}]$	(5)
mass balance of carbon	$[NaHCO_3]^0 = [HCO_3^-] + [CO_3^{2-}]$	(6)
mass balance of sodium	$[Na^+] = 2[Na_2S]^0 + [NaHCO_3]^0$	(7)
charge balance	$[Na^+] + [H^+] = 2[S^{2-}] + [HS^-] + [HCO_3^-] + 2[CO_3^{2-}] + [OH^-]$	(8)

[a] Assumptions: (1) amount of molecular H_2S and CO_2 in solution being negligible; (2) complete ionizations of aqueous Na_2S and $NaHCO_3$.
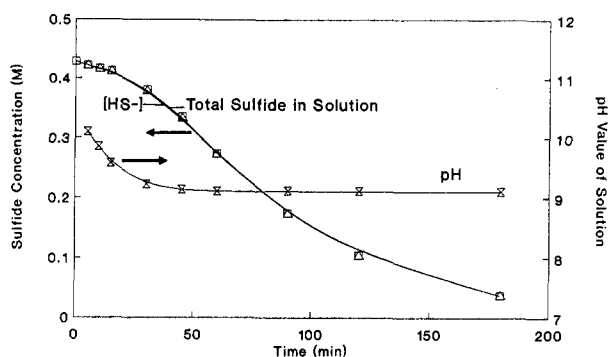
Figure 6. Measured pH, total residual sulfide and bisulfide concentrations vs reaction time (P_{CO2} = 0.121 atm; T = 35 °C; gas flow rate = 371 mL/min; $[Na_2S]°$ = 0.428 F; $[NaHCO_3]°$ = 0.6 F).
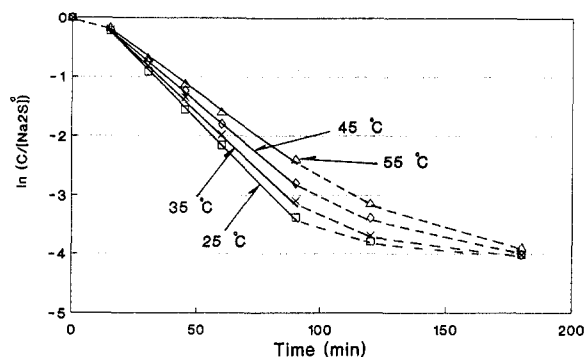
Figure 7. $\ln(C/[Na_2S]°)$ vs reaction time at different temperatures.

which corresponds to a pH value of 10.69. The measured pH value of such a solution was 10.65. This agreement suggests that the assumption of a negligible amount of molecular H_2S in solution may be acceptable; therefore, the desorption of $H_2S_{(aq)}$ may be assumed to be a fast step under the conditions studied. The observed negative effect of temperature on the overall reaction supports this argument.

After the start of the reaction, CO_2 gas was bubbled in the reactor with the release of gaseous H_2S. The mass balances of sulfur and carbon described in eqs 5 and 6 are no longer valid. However, the measured pH value of solution and the concentration of residual sulfide enable us to determine the composition of the solution. The concentration of residual sulfide measured at the end of the reaction was the total concentration of HS^- ion and aqueous H_2S. From the first dissociation constant of aqueous H_2S, the $[HS^-]$ and $[H_2S]$ can be evaluated with a measured pH of the solution. The results are plotted against time and presented as a line in Figure 6, which indicates that the sulfide exists in the solution mainly as bisulfide.

The carbonation conversion of Na_2S in our batch reactor may be divided into three periods in terms of the concentration change of sulfide in solution. As shown in Figure 7, in the early period the acidity of the solution increased rapidly but with little H_2S generation. The following reaction period was marked by the fast Na_2S conversion but with little change in the pH value of solution. As Na_2S depleted to about 90% completion, the fast conversion period tapered off to the final slow reaction period.

Concentration of H_2S in Outgoing Gas. With the knowledge of the composition of solution at various reaction times and the gas flow rate, the composition of

Table II. Average Content of H_2S in Outgoing Gas[a]

time interval (min)	av content of H_2S (%)
5-10	17.2
10-15	16.5
15-30	9.0
30-45	3.0
45-50	0.7

[a] Conditions: P_{CO_2} = 0.716 atm; T = 35 °C; $[Na_2S]$ = 0.44 M.

outgoing gas may be calculated based on the mass balances. As an example, the average partial pressures of the H_2S in outgoing gases over various time intervals are listed in Table II.

Reaction Kinetics. Figure 7 shows the plots of $\ln(C/[Na_2S]°)$ against reaction time, where C is the total sulfide concentration, for the four reaction temperatures studied. Again, it confirms the common reaction pattern mentioned before, i.e., the carbonation conversion of Na_2S to H_2S starts off with a slow reaction period, which is followed by a fast conversion period indicated by the linear regions of the plots, and finally tapers off to a slow finishing period. The similar plots for the experiments with different CO_2 flow rates and the incoming gas of different CO_2 partial pressures may be obtained, but they will not be shown here (4). In the early period in which the acidity increases rapidly, one may suggest that the following reactions take place. The Na_2S-$NaHCO_3$ solution initially is basic with a pH value about 10. Upon bubbling with carbon dioxide, a large amount of CO_2 is absorbed in the solution with little H_2S generation. The observation that gas bubbles become smaller as they rise in the solution supports this suggestion (4). The linear regions of the plots of $\ln(C/[Na_2S]°)$ vs reaction time suggest that the rate of the overall reaction is first order with respect to residual sulfide concentration. Since the majority of residual sulfide exists as an HS^- ion, it may be reasonable to conclude that it is first order with respect to the concentration of HS^- ions. The rate equation may be written as follows

$$-\frac{dC}{dt} = A_{g/l}k\frac{C}{[Na_2S]°}(P_{CO_2})^n \qquad (9)$$

where k and C are the rate constant and the sulfide concentration of the solution, respectively, and n is the order of the reaction with respect to the partial pressure of carbon dioxide in the incoming gas. Considering the error in the measurements and the physical meaning of n, one may suggest that the value of n is most likely to be unity. However, the best fitting of data available gave a value of 0.9, with a correlation coefficient of 0.999.

With the measured value of the slopes of these linear regions and the gas–liquid interfacial area, the rate constant defined above may be determined. The rate constant was found almost independent of temperature and gas flow rate in the ranges studied. It decreased slightly from 0.022 to 0.016 cm/(s·atm) when temperature increased from 25 to 55 °C and increased slightly from 0.020 to 0.022 cm/(s·atm) when the gas flow rate varied from 129 to 495 mL/min.

Since the chemical reactions in the solution are basically the transfer of protons which may be considered to be instantaneous, the possible limiting steps are believed to be those interfacial steps, in this system the absorption of carbon dioxide and the desorption of hydrogen sulfide.

Since the desorption of a dissolved gas is thermally activated, the observed negative effect of temperature on the overall reaction rate indicates that to have the desorption of hydrogen sulfide as the rate-limiting step would be inconsistent with experimental results. Hence, the absorption of carbon dioxide is most likely the rate-limiting step under the conditions studied.

V. Conclusions

Carbonation conversion of aqueous sodium sulfide to gaseous hydrogen sulfide has been found to be kinetically feasible. Furthermore, the H_2S content in the outgoing gas under the conditions studied was high enough for a Claus plant to produce elemental sulfur.

(1) In the present study, the overall reaction may proceed in three distinguishable reaction periods. Initially, the acidity of the solution increases rapidly with the absorption of CO_2. The second stage which lasts for a long period is marked by fast reactions with little change in the pH value of the solution. In the third period when the Na_2S conversion is up to about 90%, the generation of H_2S slows down.

(2) In the second period, the order of the reaction appears to be 1.0 with respect to bisulfide concentration in solution and 1.0 with respect to the CO_2 partial pressure.

(3) In the second period, the rate of the overall reaction is most likely controlled by gas/liquid reactions. The observed negative effect of temperature on the rate of overall reaction, small but definite, suggests that absorption of CO_2 not desorption of H_2S is most likely the rate-limiting step.

Nomenclature

$A_{g/l}$	interfacial area per unit volume of solution (cm^2/cm^3)
C	total sulfide concentration in solution (M)
k	constant defined by eq 9 (cm s^{-1} atm^{-1})
$K_{a1\ H_2S}$	first dissociation constant of H_2S (M)
$K_{a2\ H_2S}$	second dissociation constant of H_2S (M)
$K_{a2\ CO_2}$	second dissociation constant of CO_2 (M)
K_w	dissociation constant of water (M^2)
t	time (s)

Literature Cited

(1) Rosenquist, T. *Principles of Extractive Metallurgy*; McGraw-Hill Book Co.: New York, 1983; pp 215–225.
(2) Henold, K. L. *Chemical Principles, Properties, and Reactions*; Addison-Wesley Publishing Co.: Reading, MA, 1984; pp 610–611.
(3) Lu, W.-K.; Bryk, C.; Gou, H. Y. *Process Technol. Proc.* **1986**, *6*, 1065–1075.
(4) Ng, S. H. M.S. Dissertation, McMaster University, 1990.
(5) Miller, R. U.S. Patent No.4,588,567, May 13, 1986.
(6) Freeman, D. N.; Ciriacks, J. A.; Wehn, W. E. Efficient Recovery of Chemicals for High-Yield Sulphite-Anthraquinone Pulping, Presented at the International Sulphite Conference, Quebec, Canada, 1986.
(7) Mai, L. L.; Babb, A. L. *Ind. Eng. Chem.* **1955**, *47* (9), 1749–1756.
(8) Karchmer, J. H. *The Analytical Chemistry of Sulfur and Its Compounds, Part I*; Wiley-Interscience: New York, 1970; pp 106–107.
(9) Kolthoff, I. M.; Belcher, R. *Volumetric Analysis*; Interscience Publishing Inc.: New York, 1957, Vol. 3, pp 291–292.
(10) Nasanen, R. *Acta Chim. Fenn.* **1946**, *B19*, 90.
(11) Weast, R. C.; Lide, O. R. *CRC Handbook of Chemistry and Physics*; CRC Press Inc.: Boca Raton, 1989.
(12) Barner, H. E.; Scheuerman, R. V. *Handbook of Thermodynamical Data for Compounds and Aqueous Species*; Wiley-Interscience: New York, 1978.